

Numerical analysis on the behaviour of reinforced concrete frame structures in fire

Igor M. Džolev^{*1}, Meri J. Cvetkovska², Đorđe Ž. Lađinović¹ and Vlastimir S. Radonjanin¹

¹Department of Civil Engineering and Geodesy, Faculty of Technical Sciences, University of Novi Sad, Serbia

²Faculty of Civil Engineering, University "Ss. Cyril and Methodius", Skopje, Macedonia

(Received May 28, 2017, Revised February 8, 2018, Accepted February 9, 2018)

Abstract. Numerical approach using finite element method has been used to evaluate the behaviour of reinforced concrete frame structure subjected to fire. The structure is previously designed in accordance with Eurocode standards for the design of structures for earthquake resistance, for the ductility class M. Thermal and structural response are obtained using a commercially available software ANSYS. Temperature-dependent nonlinear thermal and mechanical properties are adopted according to Eurocode standards, with the application of constitutive model for the triaxial behaviour of concrete with a smeared crack approach. Discrete modelling of concrete and reinforcement has enabled monitoring of the behaviour at a global, as well as at a local level, providing information on the level of damage occurring during fire. Critical regions in frame structures are identified and assessed, based on temperatures, displacements, variations of internal forces magnitudes and achieved plastic deformations of main reinforcement bars. Parametric analyses are conducted for different fire scenarios and different types of concrete aggregate to determine their effect on global deformations of frame structures. According to analyses results, the three-dimensional finite element model can be used to evaluate the insulation and mechanical resistance criteria of reinforced concrete frame structures subjected to nominal fire curves.

Keywords: fire resistance; RC frame structure; numerical analysis; transient fire response

1. Introduction

A numerical approach in determining the performance of reinforced concrete structures subjected to fire has been rapidly increasing with the development of computer systems. As an alternative to fire tests, which provide the most accurate data, but are often expensive and restricted by the furnace size, prognostic models using neural networks (Lazarevska *et al.* 2012) and specialized software based on Finite Element Method (FEM), such as SAFIR (Talamona and Franssen 2005, Tan and Nguyen 2013), VULCAN (Huang *et al.* 2006) and OPENSEES (Jiang and Usmani 2013, Jiang *et al.* 2011), are being developed at the universities and other research facilities, to simulate the behaviour of structures in case of fire. Also, some powerful commercial software, such as ANSYS (Ding and Wang 2008, Dwaikat and Kodur 2013, Hawileh and Naser 2012, Hawileh *et al.* 2009, Kodur *et al.* 2013, Zhou and Vecchio 2005) and ABAQUS (Bailey and Ellobody 2009, Ellobody and Bailey 2009, Gao *et al.* 2013, Mirza and Uy 2009) have been used and validated by the performed test results. Due to the complexity of the calculation, all of the above mentioned software, have the capability to perform nonlinear calculations, both thermal and mechanical.

According to EN 1992-1-2 (2004), a structure can be evaluated at three levels of increasing complexity and size.

While members and some substructures can be tested in numerous facilities, large scale tests on global structures so far are very rare (Lennon and Moore 2003), resulting in a global structural analysis performed mostly using advanced calculation methods. Although a plane frame structure is analysed, due to a nature of fire action, a 3D model is developed, consisting of solid and line elements representing concrete and reinforcement, respectively, to account for a spatial heat transfer and a more realistic assessment of degradation of mechanical properties at a cross-section level.

2. Advanced calculation methodology

The first calculation step in assessing the fire resistance of the structure, is to determine the thermal response in the form of time-dependent temperature distribution throughout the structural elements. Temperature fields in the elements during fire exposure depend on the design fire model, as well as on the temperature-dependent thermal and physical properties of concrete and steel reinforcement. Due to high temperatures in case of fire, in addition to conduction and convection, radiation should also be considered, as described in EN 1991-1-2 (2002).

In software ANSYS® (2015), thermal and stress analysis are not fully coupled. First, thermal calculation is carried out for the entire duration of the fire, after which the structural analysis is performed, taking into account the temperature variation in time along the elements.

Validation of the results obtained using this procedure

*Corresponding author, Ph.D. Student
E-mail: idezolev@uns.ac.rs

has shown that the deformation of elements can be reasonably accurately predicted providing that the load induced thermal strain (LITS) is incorporated into the model. (CEB-FIP 2007) The stress-strain curves for concrete provided in EN 1992-1-2, implicitly account for the transient creep strain. One of the major limitations of implicit models concerns the unloading stiffness at elevated temperatures. The mechanical strain given by implicit models for a given stress-temperature state is the same, whether concrete has been heated and then loaded at constant temperature or loaded and then heated under constant stress, which does not correspond to experimental evidence. A formulation of the EN 1992-1-2 concrete model at elevated temperatures that includes an explicit term for transient creep has been proposed by Gernay and Franssen (2012) and implemented in the software SAFIR. Experimental tests on large scale models have shown that the cooling phase (thermal unloading) is of crucial importance for the behaviour of structures, especially in cases where thermal expansion is restrained, and therefore, the explicit model is particularly recommended when modelling the cooling phase of a fire (parametric and real fire models, which are not covered in this paper).

Structural analysis is performed in two steps. First, mechanical load is applied and the behaviour of the structure is assessed prior to fire action. In the second step, the deformed structure with initial pre-stress condition resulting from mechanical actions is exposed to thermal loads, previously calculated in the transient thermal analysis, at specific time points, throughout the whole duration of the fire. Since standard ISO 834 (1975) fire curve is applied, which is monotonically increasing, the main objective of the analysis is to assess the fire resistance of elements and the whole system in terms of time, and the ability to retain and limit the fire spread within the fire sector.

3. Finite element model development

The analysis is carried out using finite element software ANSYS Workbench 16.0. The constitutive material models for concrete and steel are adopted according to EN 1992-1-2, while the thermal action is defined using standard ISO 834 fire curve. The sequentially coupled thermo-mechanical analysis procedure requires two models with a same geometry to be developed: the first to be used in transient thermal analysis, to evaluate the thermal response of the structure, and the second to be used in a transient structural analysis, where mechanical and thermal loads are used to obtain the physical response of the structure.

3.1 Modelling assumptions

The following assumptions are made in the development of the numerical model:

- Bond-slip between steel reinforcement and concrete is not taken into account. Perfect bond is assumed, resulting in equal total strain in the reinforcement and concrete in the contact region. While inclusion of the interfacial behaviour leads to more accurate predictions,

the effect may be ignored (although un-conservative for steel temperature above 500°C (Huang 2010)), when the objective of the analysis is to obtain the global response of the structure. (Gao *et al.* 2013)

- Transient creep strain in concrete is modelled implicitly, according to EN 1992-1-2 concrete model. Since cooling phase is not considered, this would not affect the overall behaviour of the structure.
- Fire induced spalling is not considered in the analysis. Ordinary performance concrete usually resists rapid heating rates with only minor spalling or even without spalling. (Klingsch 2014) As a low moisture level is assumed, and the analysis is focused on a normal strength concretes with higher porosity and permeability than e.g., in high strength concretes, high pore pressures that might lead to failure due to explosive spalling are avoided.

3.2 Thermal model development

For the thermal analysis, geometry of the structure is discretized using 8-node 3D SOLID70 element and a uniaxial 2-node line element LINK33, for concrete and reinforcing steel, respectively, with a single degree of freedom at each node point, temperature. Different mesh densities are used for thermal and structural model. Since heat transfer is dominant throughout the cross-section and is practically constant along the element, to avoid using large time-steps or the appearance of space oscillations of the solution, in case of thermal shock (Bergheau and Fortunier 2008), mesh element size is adopted as $\Delta x = 1.25$ cm, resulting in a total number of 1.120.908 elements. A tie constraint is used to apply temperatures from concrete to reinforcing steel bars at the coinciding node locations. Surface elements SURF152 are used to apply thermal load in terms of convection and radiation. Convection coefficients $\alpha_c = 25 \text{ Wm}^{-2}\text{°C}^{-1}$ and $\alpha_r = 9 \text{ Wm}^{-2}\text{°C}^{-1}$ are adopted for exposed and unexposed surfaces, respectively, while emissivity related to concrete surface is adopted as $\epsilon_m = 0.7$.

3.3 Structural model development

Concrete is modelled using 8-node 3D SOLID65 element, with three degrees of freedom at each node: translations in the nodal x , y , and z directions. Concrete material is modelled using nonlinear constitutive concrete material model of William and Warnke (1974), combined with multilinear isotropic hardening plasticity, following stress-strain curves provided in EN 1992-1-2. The element is capable of cracking in tension and crushing in compression. Cracking is permitted in three orthogonal directions at each integration point. The presence of a crack at an integration point is represented through modification of the stress-strain relations by introducing a plane of weakness in a direction normal to the crack face. The open and close crack shear transfer coefficients, β_t and β_c , representing the amount of shear force transferred through opened and closed crack are adopted as 0.4 and 0.8, respectively (0 indicating smooth crack with a total loss of shear transfer and 1 indicating rough crack without any loss

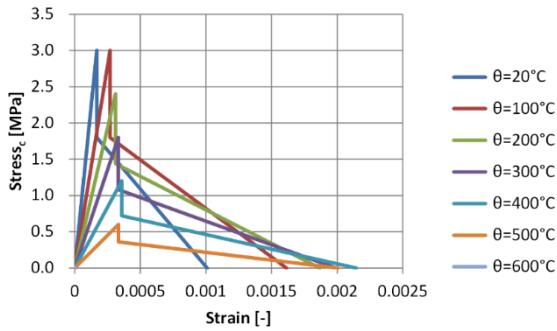


Fig. 1 Temperature-dependent tensile strength of concrete C30/37

of shear transfer). Tensile behaviour of concrete before cracking is assumed to be linear elastic. In the tension zone, Thelandersson (1982) assumes brittle fracture after crack formations. According to Gao *et al.* (2013), Bazant and Oh (1983), using the crack band model approach, the tensile stress within the crack band gradually decreases while the strain increases (stress softening). It is presented by a sudden reduction of the tensile stress to $0.6f_{t_r}$, and a linear descending to zero stress at a strain of $6\varepsilon_{cr}$ (Fig. 1). If the material at an integration point fails in uniaxial, biaxial, or triaxial compression, it is assumed to crush at that point, leading to a complete deterioration of the structural integrity of the material, with a neglected contribution to the stiffness of an element at the integration point.

Modelling of reinforcement can be achieved using discrete (explicit) or smeared (implicit) approach. The latter can be implemented through the SOLID65 element as a real constant, which smears the stiffness of reinforcement over the concrete element. Discrete approach implies that each reinforcement bar is modelled as a separate body. Steel reinforcement is modelled as a uniaxial 2-node line element LINK180, with 3 translational degrees of freedom at each node. The nodes of the reinforcement and the surrounding concrete elements coincide and are coupled. Multilinear isotropic hardening plasticity is assumed, since large strains are expected to develop. General structural model mesh size is adopted as $\Delta x=5.0$ cm, except in the regions of severe thermal gradients (concrete cover), where element size is

reduced to $\Delta x=2.5$ cm, leading to a total of 34.839 elements.

Mechanical properties of concrete and steel used to generate nominal stress-strain-temperature relations are converted into true stress-strain curves, to account for dimensional changes and to provide more realistic representation of the material behaviour (Pakala and Kodur 2016), using following relations:

$$\sigma_{true} = \sigma_{nom}(1 + \varepsilon_{nom})$$

$$\varepsilon_{true} = \ln(1 + \varepsilon_{nom})$$

3.4 Model validation

Full scale tests on reinforced concrete frame structures are very rare. The above finite element model is validated by comparing predicted thermal and structural response with measured data in fire tests performed by Dwaikat and Kodur (2009) and numerical model developed in ABAQUS by Kodur and Agrawal (2016). The beam is made of normal strength concrete and no spalling was observed during fire exposure. Geometry of the beam and reinforcement layout, as well as loading and boundary conditions are presented in Fig. 2. Finite element model mesh for concrete and reinforcement elements of the 1/4 of the beam is presented in Fig. 3. A two-plane symmetry is used to model the beam, significantly reducing the computational time.

The beam is loaded using two point loads, which remained constant during the subsequent fire exposure. The beam is subjected to a standard fire (ASTM E-119-08a 2008) from three sides, bottom and side surfaces, in the region between the compartment walls. The predicted and measured temperatures in concrete and reinforcement rebar are presented in Fig. 4.

Temperatures obtained using numerical procedures in ANSYS and ABAQUS are very similar and show good agreement with measured results. Differences can be observed in the first 30-60 minutes, with numerical models predicting lower temperatures than measured, resulting in a slower degradation of mechanical properties and expected smaller deflections of the beam mid-span. Deflection prior to fire exposure is selected as the initial condition for the deflection of the beam during fire (Fig. 5).

After 130 minutes, beam stiffness starts to reduce more

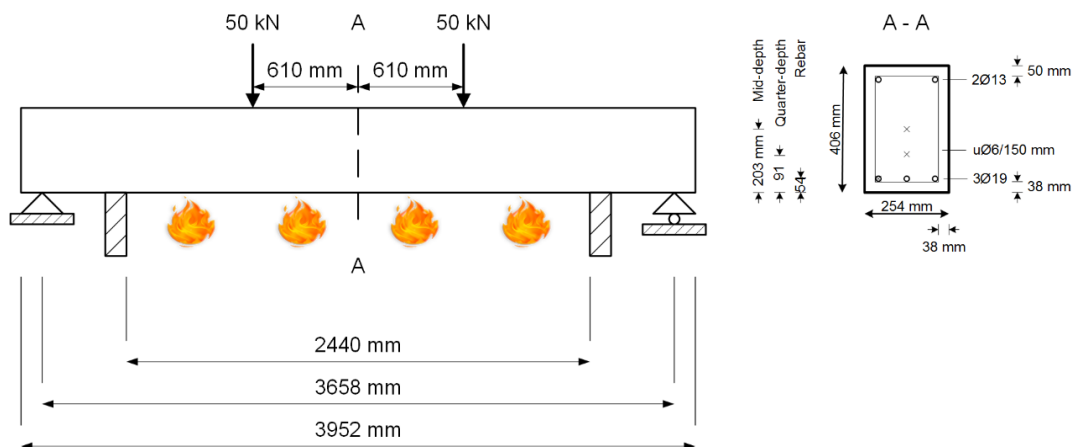


Fig. 2 Tested beam used in validation of the developed finite element model

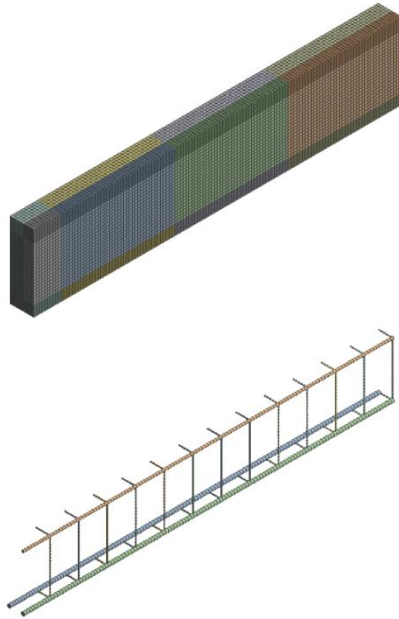


Fig. 3 Finite element mesh for concrete and reinforcement elements of the developed 1/4 of the beam FE model using two-plane symmetry

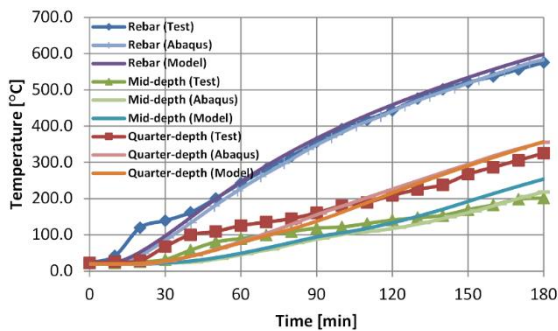


Fig. 4 Measured and predicted temperatures using ABAQUS and ANSYS

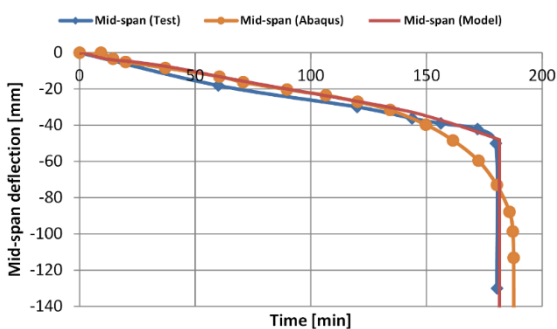


Fig. 5 Measured and predicted mid-span deflection using ABAQUS and ANSYS

rapid in ABAQUS model, while the model developed in ANSYS shows better agreement with measured data, until failure at around 180 minutes of fire.

4. Reinforced concrete frame structure exposed to standard ISO 834 fire

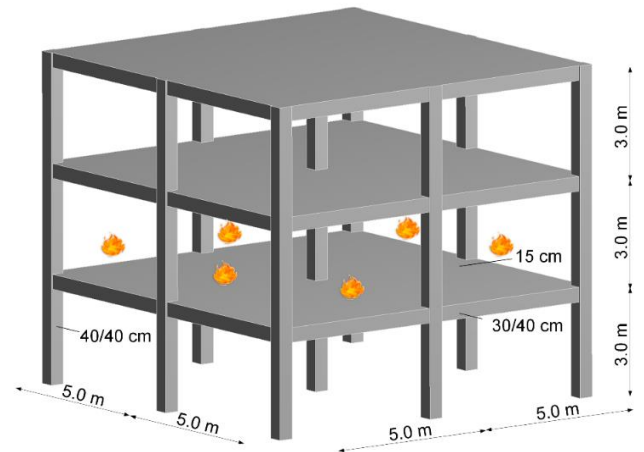


Fig. 6 Reinforced concrete structure geometry

4.1 Model geometry, loading and boundary conditions

A three-story two-bay reinforced concrete structure designed for ductility class M, according to EN 1998-1-1 (2004) is subjected to standard ISO 834 fire (Fig. 6).

Since the structural geometry is two-plane symmetrical, only central plane frame is analysed. To account for a spatial heat distribution, resulting in a heat transfer in plane as well as perpendicular to the plane of the frame, 3D model of the plane frame is developed. Fire analysis accounts for total permanent load and 50% of imposed load. Fire limit state load, model geometry and adopted reinforcement are presented in Fig. 7. Concrete grade C30/37 mixed with siliceous aggregate and reinforcement S500 type C, are considered in the design. Since the fire sector is assumed to cover the entire single floor area, two-plane symmetry is used to model the structure, reducing the number of elements by approximately 75% and thus, significantly reducing the computational time.

Unlike structural model geometry, model geometry for thermal analysis includes a part of the floor concrete slab, to account for heat transfer in more realistic approach. Also, since the slab represents the physical barrier that restricts the fire compartment, the temperature development on unexposed slab surface can be used to assess the insulation criteria of the frame structure. Effect of slabs is neglected in the structural analysis. Lateral restraint of slabs is provided only by the shear resistance of the perimeter columns, arguing about the magnitude of the influence of membrane actions on the remaining frame structure.

4.2 Thermal response of the structure

Temperature profiles are constant along the element. Thermal response of concrete members has been previously validated (Džolev *et al.* 2016) based on Annex A of EN 1992-1-2. The arbitrary cross-section response of columns (1/4 of the cross-section) exposed to all four sides and beams (1/2 of the cross-section) separating fire sector from the rest of the structure, is presented in Fig. 8.

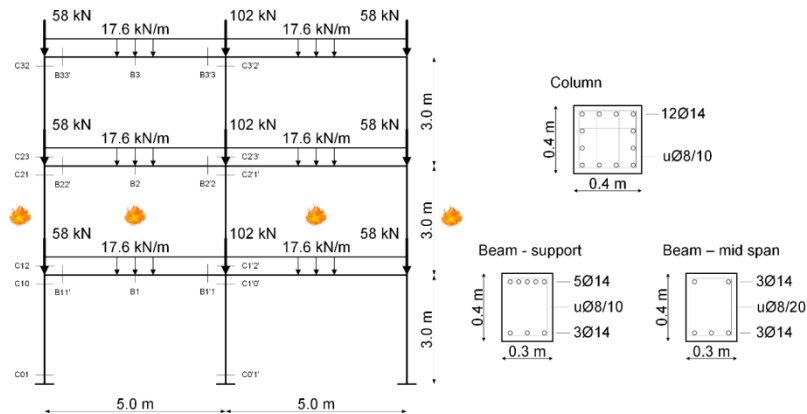


Fig. 7 RC frame geometry, load and adopted reinforcement

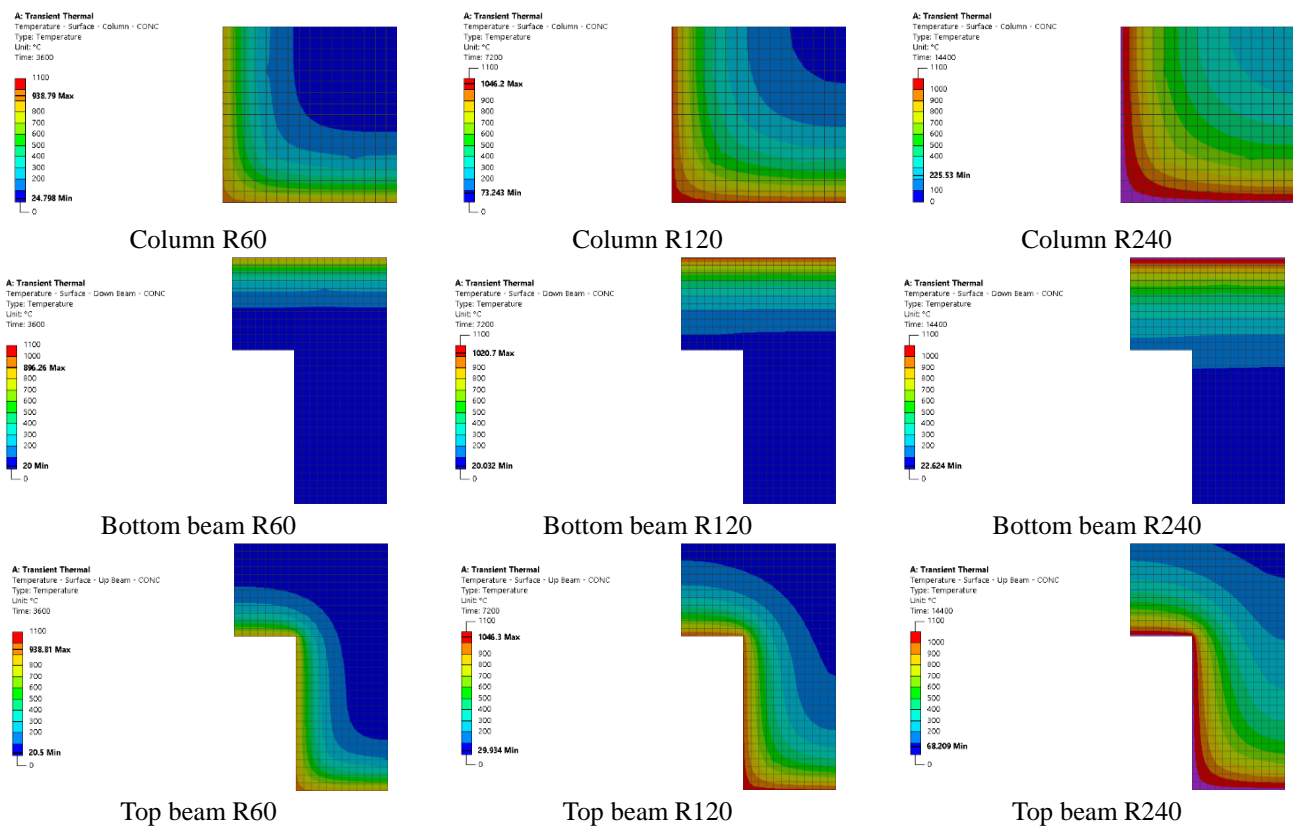


Fig. 8 Temperature profiles of columns and beams surrounding the fire sector

Temperature histories of main reinforcing bars in column and beam elements are presented in Figs. 9-11. Thermal conductivity of concrete is relatively low compared to steel, providing very good thermal insulation to the reinforcement. After 1 and 2 hours of fire duration, maximum surface temperatures of exposed concrete members are 938°C and 1046°C, respectively, while maximum reinforcement temperatures are observed in the corner reinforcement bars of the corresponding member surfaces and amount to 313°C and 538°C, respectively. Reinforcement protection can only be assured under assumption that concrete spalling does not occur. In the first 30 minutes of fire exposure, thermal gradient in the concrete cover zone is the highest, resulting in large tensile stresses induced by thermal expansion that lead to severe

cracking of concrete. Mild deviation of the reinforcement temperature at around 750°C is a consequence of the peak values in the specific heat of steel in the temperature range of 700-800°C. Temperature of the main reinforcement bars positioned in the unexposed zone of the beam members gradually increases, but remains relatively low, assuring full load bearing capacity of reinforcement. Temperature distribution in time of the unexposed slab surface is presented in Fig. 12. The insulation criteria of the concrete slab with a depth of 15 cm is assumed to be satisfied for the period of time where the average temperature rise of the unexposed surface is limited to 140°C. Since the ambient temperature is assumed at 20°C, the limiting temperature value of 160°C is used to determine fire resistance class of the insulation criteria, resulting in 247 minutes.

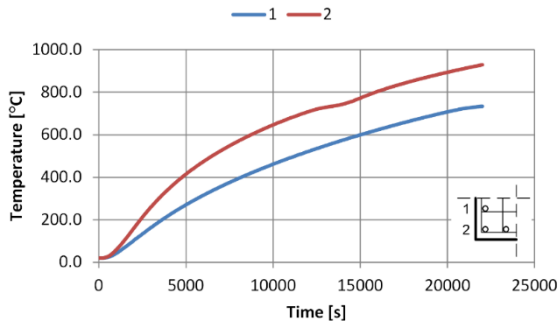


Fig. 9 Temperature evolution in Column 2 reinforcement

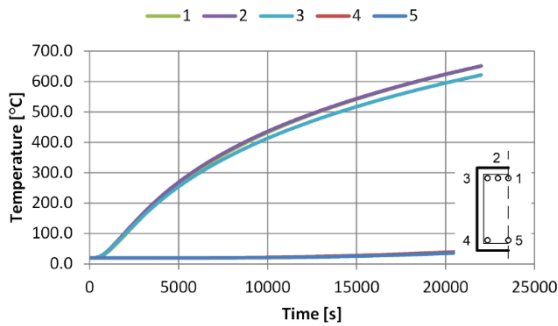


Fig. 10 Temperature evolution in Beam 1 reinforcement

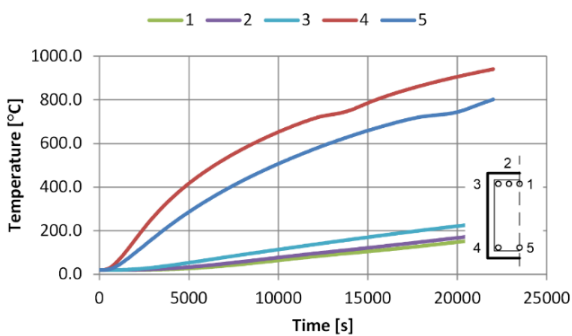


Fig. 11 Temperature evolution in Beam 2 reinforcement

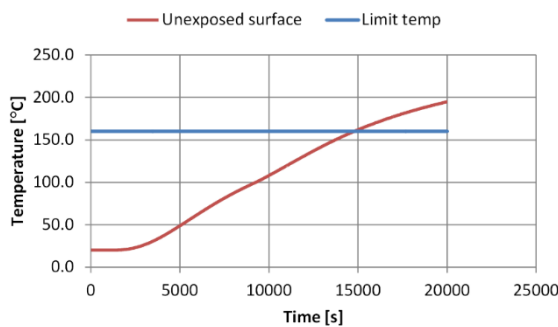
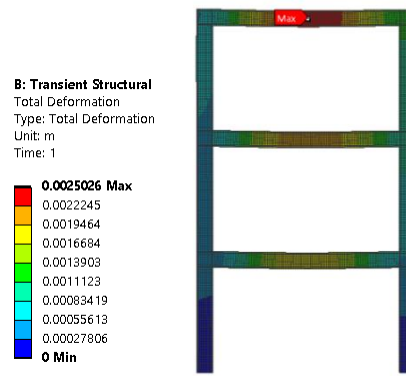


Fig. 12 Fire resistance of the slab for the insulation criterion

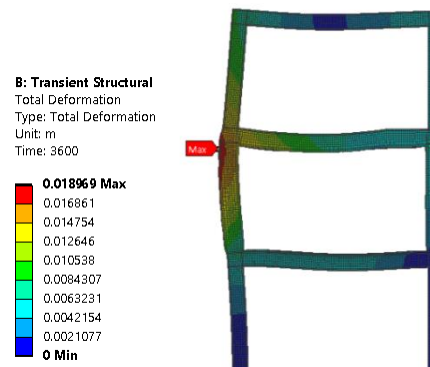
4.3 Structural response of the structure

4.3.1 Structural displacements

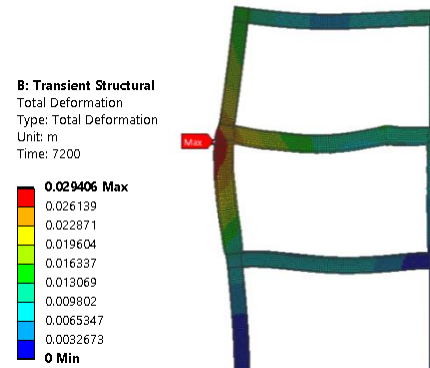
Elevated temperatures in RC members introduce thermal strains and degradation of material mechanical properties. Thermal expansion and gradual decrease of the frame stiffness result in increased deformation of members. Total deformation prior to fire, after 60, 120 and 240



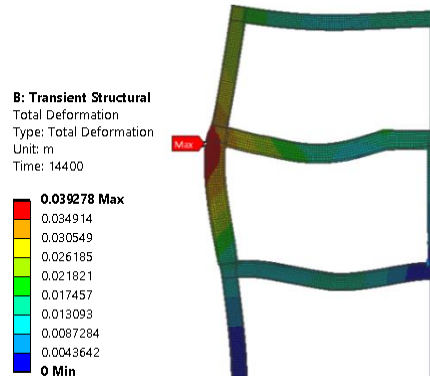
(a) Prior to fire



(b) After 60 minutes of fire



(c) After 120 minutes of fire



(d) After 240 minutes of fire

Fig. 13 Total deformation of frame during standard fire

minutes of fire duration is presented in Fig. 13. The largest deformations are observed in the members directly exposed to fire.

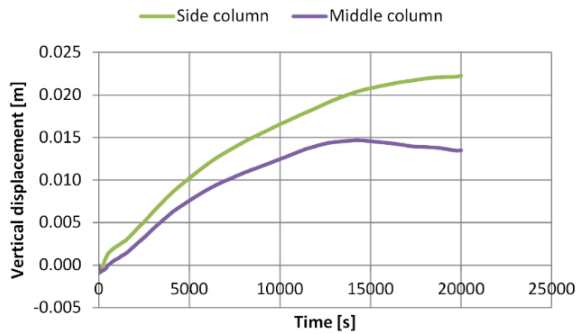


Fig. 14 Vertical displacement at the top of fire exposed columns

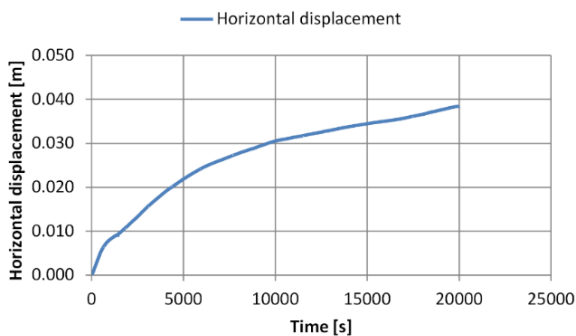


Fig. 15 Maximum horizontal displacement

Vertical displacement at the top of the middle and side columns exposed to fire is presented in Fig. 14. Columns initially extend upwards due to thermal expansion, but as the strength and stiffness are reduced with higher temperatures, after 240 minutes, middle column vertical thermal expansion becomes smaller than the deformation from the applied external load, resulting in the total vertical displacement moving downwards.

Evolution of maximum horizontal displacement is presented in Fig. 15. Horizontal displacement is governed by the thermal expansion of heated beams and shear resistance of columns. It can be observed that the rate of displacement is reduced in time as the beam softens.

4.3.2 Axial forces and bending moments

Reduction of axial stiffness can be observed on the diagram of axial forces in the beam section B2'2. The heated beam tends to expand as the temperature rises, but as the column imposes a restraint effect, the axial force in the beam rises and reaches peak level of about 80 kN (compression, 8 times higher than the ambient value), at 65 minutes of fire exposure (Fig. 16). Axial force then starts to decline, due to degradation of concrete material and a reduction of axial stiffness of the beam.

Since thermal expansion of the heated parts is partially restrained, compression is rising in concrete areas exposed to thermal action, resulting in shifting of bending moment diagrams in the direction of heat transfer, as presented in Fig. 17. Upper beam (Beam 2) bending moments become negative after 6 minutes, while lower beam (Beam 1) bending moments become all positive at 50 minutes of fire exposure. Shifting of bending moments could potentially

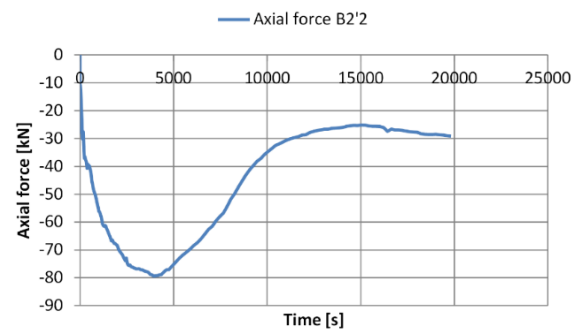


Fig. 16 Axial force in cross-section B2'2

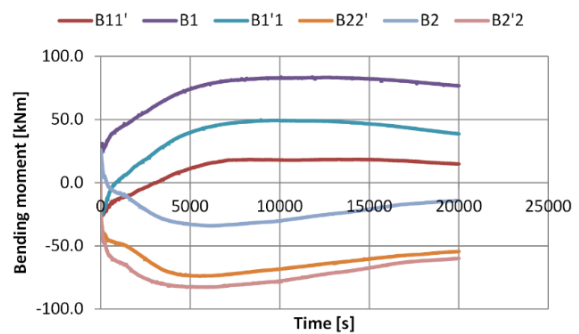


Fig. 17 Evolution of bending moments of exposed beams at specific cross-sections

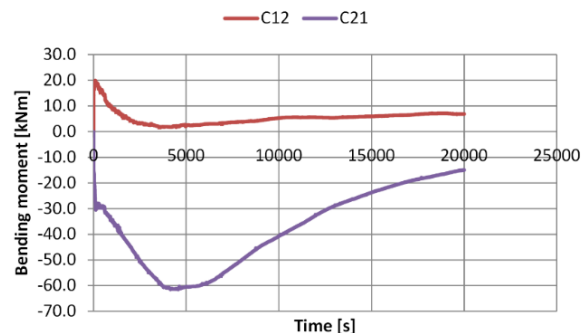


Fig. 18 Evolution of bending moments of exposed side column at specific cross-sections

lead to an early failure if the cross-section bending capacity is exceeded (sections B1, B22' and B2'2). Particular attention should also be given to the zones where moment changes sign (B11', B1'1 and B2) since these sections were not designed taking into account this possibility. Absolute maximum moment values in the sections B1, B22' and B2'2 are 3.19, 2.83 and 3.12 times higher, respectively, than prior to fire exposure.

Axial force in the columns practically remains constant during time. Distribution of bending moments in Column 2 at the cross-sections C12 and C21 are presented in Fig. 18. Absolute maximum bending moment at a C21 section peaks at 70 minutes of fire exposure and reaches 4 times higher values than before the fire.

4.3.3 Mechanical response of reinforcement

Load bearing capacity of steel reinforcement begins to decline after exceeding 400°C, at about 80 minutes of fire

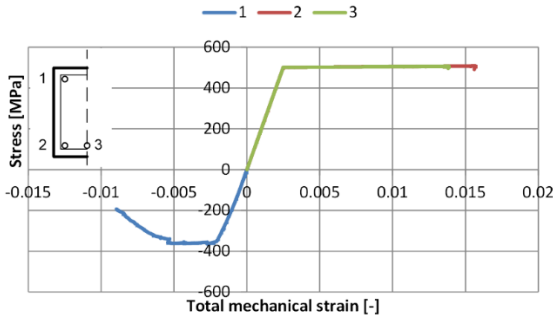


Fig. 19 Stress-strain curves of reinforcement bars in the B1 section

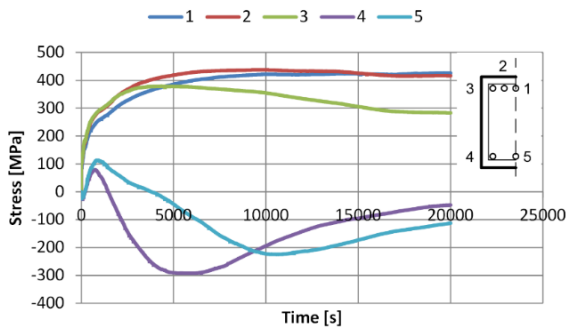


Fig. 20 Stress-time curves of reinforcement bars in the B2'2 section

exposure for corner bars of exposed elements. Stress-strain curves of reinforcing bars in the section B1 is presented in Fig. 19. Plastic strains start to develop after 80 minutes, first in the heated top corner bars, followed by yielding of bottom corner and middle bars at 111 and 125 minutes, respectively, whose temperatures remain slightly above ambient, assuring full load bearing capacity. Initially compressed bottom reinforcement in the B2'2 section is transferred to tension after 3 minutes of fire exposure, due to thermal expansion of concrete cover zone. Tension is increased for the next 10 minutes, after which stress starts to decline. After 24 and 63 minutes of fire exposure, corner and middle bar, respectively, changes from tension back to compression. Stresses reach peak values at 85 minutes in corner bars and 170 minutes in the middle bar. Evolution of stresses is presented in Fig. 20. Plastic deformation of bottom bars starts at 76 minutes for corner bars and 202 minutes for middle bar. Since yielding of steel at elevated temperatures occurs at a total mechanical strain of 2%, it can be observed that yielding does not occur (Fig. 21), although load bearing capacity of bottom reinforcement is highly reduced at higher temperatures. Stress-strain diagrams for reinforcement bars in the section B2'2 are presented in Fig. 22. Critical cross-section in the Beam 2 is not located at the end of the beam or in the middle, as expected, but at a section where additional top reinforcement bars, at a distance of 1 m from the middle column, are no longer required. Suspension of additional reinforcement results in a redistribution of stresses to a corner bar, eventually exceeding its load bearing capacity and causing it to yield (Fig. 23).

Although exposed columns are heated from all four

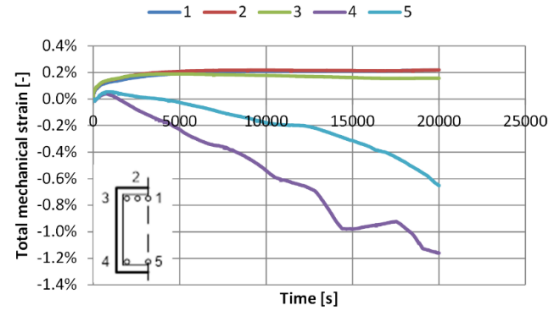


Fig. 21 Evolution of total mechanical strain in reinforcement bars in the B2'2 section

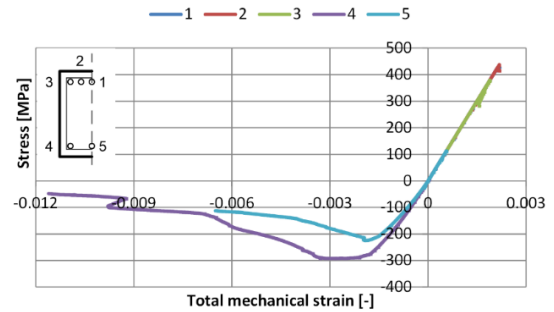


Fig. 22 Stress-strain curves of reinforcement bars in the B2'2 section

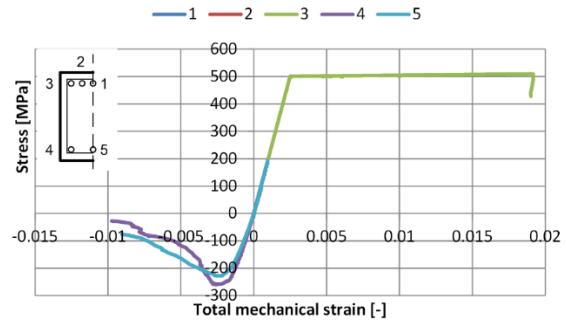


Fig. 23 Stress-strain curves of reinforcement bars in the critical Beam 2 section

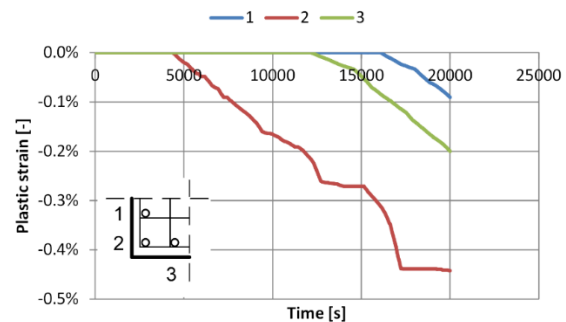


Fig. 24 Evolution of plastic strains in reinforcement bars in the C2'1' section

sides, resulting in high temperatures in all main reinforcement bars, total mechanical strains in time are far below the arbitrary 2%. Plastic strains start to develop in corner bars after 73 minutes, and in side bars after 202 and 268 minutes, but yielding of bars does not occur (Fig. 24).

Table 1 Parametric study of the influence of fire scenario and concrete aggregate type

Analysis label	Fire on ground floor	Fire on 1 st floor	Fire on 2 nd floor
Calcareous aggregate	P105C	P205C	P305C
Siliceous aggregate	P105S	P205S	P305S

5. Effect of different fire scenarios and concrete aggregate type

Fire sector is assumed to cover the entire floor area. In order to study the effect of different fire scenarios on the response of frame structures, position of fire is migrated covering one floor at a time. When designing RC structures, mechanical properties of concrete are adopted according to concrete grade. The same concrete grade can be achieved using various aggregates, but the influence of the type of aggregate on the behaviour of RC frame structures at elevated temperatures is reflected in different thermal expansions of siliceous and calcareous aggregates, as well as in stress-strain relations for concrete, according to EN 1992-1-2 (2004). A total of six analysis are conducted (Table 1).

Since thermal response of beams and columns depends on the type of fire exposure and material and geometrical properties of exposed elements, temperature fields are translated according to scenario. Each floor geometry is the same, resulting in same thermal response relative to fire position.

Mechanical response depends not only on the temperature fields, but also on the level of stresses and strains developed in members prior to fire exposure and on the restraining effects of the surrounding elements. Fig. 25 presents maximum horizontal displacements after 1, 2, 3 and 4 hours of standard fire exposure depending on the fire scenario and the type of aggregate.

For the same fire scenario, horizontal displacements are 5 to 13% larger for concrete made with siliceous aggregate compared to calcareous, due to larger thermal expansion and more rapid compressive strength reduction at elevated temperatures. Relative horizontal displacements in case of fire covering the 1st floor compared to fire on the ground floor are 12-13% larger in case of calcareous aggregate and 14-15% larger in case of siliceous aggregate. This difference is maintained uniform as the fire continues, unlike relative displacements when comparing fire on the 2nd floor to the fire on the 1st floor, where the difference after 1, 2, 3 and 4 hours is approximately 5, 7, 12 and 21%, respectively, with 1-2% larger difference in case of calcareous aggregate. Larger relative increase in horizontal displacements in time can be attributed to the column-beam joint rotation, which, in case of fire on the last floor, is governed only by the stiffness of connected heated elements, and not the surrounding cooler part of the structure that would provide additional restraining effect.

The largest relative deflections are observed in beams surrounding fire sector from the top and are approximately 40-130% greater than in beams surrounding fire sector from

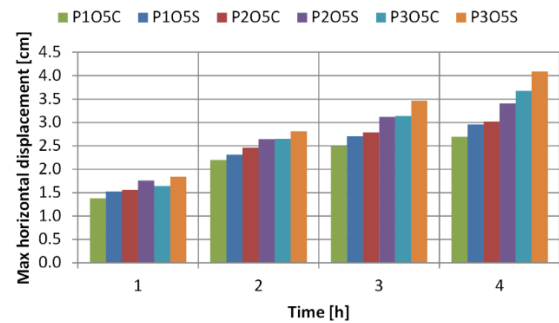


Fig. 25 Maximum horizontal displacements

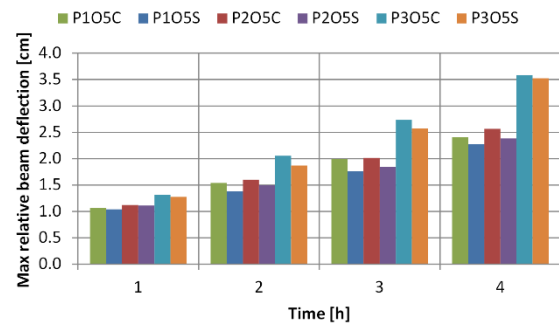


Fig. 26 Maximum relative deflections of beams

the bottom. This is expected, since top beams are exposed to fire from bottom and side surfaces, providing faster temperature rise in elements, unlike bottom beams, which are exposed only from the top. Deformation of the frame structure below the position of the fire is of much lower magnitude than above it, providing practically constant deflection of Beam 1 in case of fire on the 2nd floor. On the contrary, deformation of the structure above the fire sector depends on the deformation of elements surrounding the fire sector and consists to a large extent of a rigid body movement. Maximum relative deflections of beams are presented in Fig. 26. For the same fire scenario, beams made with siliceous aggregate experience 1 to 11% smaller deflections compared to calcareous aggregate, as opposed to horizontal displacements. As the fire position is moved upwards, maximum beam deflections are increased by 1 to 8% in case of fire on the 1st floor. In case of fire on the 2nd floor, after first hour of exposure, maximum deflections are 15 to 17% larger compared to the fire on the 1st floor, but as the fire exposure continues, the difference is getting larger, up to 39% and 47%, for concrete made with calcareous, compared to siliceous aggregate, respectively.

5. Conclusions

A nonlinear finite element analysis on the behaviour of reinforced concrete frame structure was conducted. The frame was designed according to EN 1998-1-1, for the ductility class M, and subjected to standard ISO 834 fire, covering the entire floor area. Influence of different fire scenarios was considered, as well as different types of concrete aggregate. Material input data for concrete and steel at elevated temperatures were adopted according to

EN 1992-1-2. Commercial software ANSYS was used to determine both thermal and mechanical response of the structure, using two separate models. Based on the results of analyses, the following conclusions can be made:

- ANSYS can be used to evaluate response of RC frame structures, taking into account nonlinear thermal and mechanical temperature-dependant properties of both concrete and steel.
- RC frame structure designed according to EN 1998-1 has proved to be very resistant in case of fire, providing insulation and load bearing function for sufficient period of time.
- Bending moment diagrams of fire exposed members shift during fire in the direction of heat transfer, identifying potential critical regions where extreme bending moments reach values up to 4 times higher than initial. These include mid-span sections of beams exposed to fire from the top, and end sections of beams exposed from the bottom, as well as top cross-sections of exposed side columns. Special consideration should be applied to the sections where discontinuity of main reinforcement bars according to layout is presented, reducing the cross-section moment capacity.
- While the variation of axial force in the exposed beams reaches 8 times larger values than at ambient temperature, axial force in the columns remain practically constant.
- Concrete cover is crucial for protecting the main reinforcement bars in terms of prolonging the temperature rise, which leads to degradation of mechanical properties of steel. Special attention should be paid for assuring that concrete spalling is prevented.
- Due to large thermal gradient in the first 15 minutes of fire, expansion of concrete cover is causing tension in initially compressed reinforcement. After reaching maximum values, stress in reinforcement is reduced due to degradation of concrete cover, and compressive stress starts to develop again, eventually causing plastic deformation of compressed reinforcement.
- Stress reduction in more heated reinforcement bars results in stress redistribution to the surrounding bars of a lower temperature and, thus, higher load bearing capacity. Yielding of tensile reinforcement occurs near the mid-span of a beam exposed to fire from the top surface and in the section near the end of the beam exposed to fire from the bottom, in the vicinity of central column. Bars that yielded are positioned opposite to fire exposed beam surfaces, remaining in the cooler part of the beam section.
- Although plastic deformations of column reinforcement developed, yielding did not occur. Probable reason for this lies in the design procedure according to EN 1998-1, to prevent plastic hinge formation in columns due to seismic action, making them more resilient to incidental actions, in general.
- As the fire position is migrated to higher floors, deformations of elements are increased. The largest deformations are observed in elements surrounding the fire sector. Global damage of the structure is concentrated at the level of fire and consequently above it, while below it, minor damage is observed.

- Depending on the type of aggregate, larger horizontal displacements are observed in case of siliceous aggregate, while maximum relative beam deflections are larger in case of calcareous aggregate. In all cases analysed, deformations of elements due to different type of aggregate differ by maximum 13%.

Acknowledgments

The research has been conducted within the scientific research project TR 36043, funded by the Ministry of Science of Serbia. The authors would like to thank Faculty of Civil Engineering in Subotica, University of Novi Sad, for the ceded license for ANSYS Academic product.

References

- ANSYS® Academic Teaching Mechanical (2015), ANSYS Help Documentation, Release 16.0, ANSYS, Inc., Canonsburg.
- ASTM E-119-08a (2008), Standard Test Methods for Fire Tests of Building Construction and Materials, American Society for Testing and Materials, USA.
- Bailey, C. and Ellobody, E. (2009), "Whole-building behaviour of bonded post-tensioned concrete floor plates exposed to fire", *Eng. Struct.*, **31**, 1800-1810.
- Bažant, Z. and Oh, B. (1983), "Crack band theory for fracture of concrete", *Mater. Struct.*, **16**, 155-177.
- Bergheau, J.M. and Fortunier, R. (2008), *Finite Element Simulation of Heat Transfer*, John Wiley & Sons, Inc., Hoboken, USA
- CEB-FIP (2007), Fire Design of Concrete Structures-Materials, Structures and Modelling (T. Bulletin 38), International Federation for Structural Concrete (fib), Lausanne, Switzerland.
- Ding, J. and Wang, Y. (2008), "Realistic modelling of thermal and structural behaviour of unprotected concrete filled tubular columns in fire", *J. Constr. Steel Res.*, **64**, 1086-1102.
- Dwaikat, M. and Kodur, V. (2009), "Response of restrained concrete beams under design fire exposure", *J. Struct. Eng.*, **135**(11), 1408-1417.
- Dwaikat, M. and Kodur, V. (2013), "A simplified approach for predicting temperatures in fire exposed steel members", *Fire Saf. J.*, **55**, 87-96.
- Džolev, I., Cvetkovska, M., Ladinović, Đ., Radonjanin, V. and Rašeta, A. (2016), "Fire analysis of a simply supported reinforced concrete beam using Ansys Workbench", *8th Symposium 2016 Association of Structural Engineers of Serbia*, Zlatibor, September.
- Ellobody, E. and Bailey, C. (2009), "Modelling of unbonded post-tensioned concrete slabs under fire conditions", *Fire Saf. J.*, **44**, 159-167.
- EN 1991-1-2 (2002), Actions on Structures, General Actions, Actions on Structures Exposed to Fire, European Committee for Standardization, Brussels, Belgium.
- EN 1992-1-2 (2004), Design of Concrete Structures, General Rules, Structural Fire Design, European Committee for Standardization, Brussels, Belgium.
- EN 1998-1-1 (2004), Design of Structures for Earthquake Resistance: General Rules, Seismic Actions and Rules for Buildings, European Committee for Standardization, Brussels, Belgium.
- Gao, W., Dai, J.G., Teng, J. and Chen, G. (2013), "Finite element modeling of reinforced concrete beams exposed to fire", *Eng. Struct.*, **52**, 488-501.

- Gernay, T. and Franssen, J.M. (2012), "A formulation of the Eurocode 2 concrete model at elevated temperature that includes an explicit term for transient creep", *Fire Saf. J.*, **51**, 1-9.
- Hawileh, R. and Naser, M. (2012), "Thermal-stress analysis of RC beams reinforced with GFRP bars", *Compos. Part B*, **43**, 2135-2142.
- Hawileh, R., Naser, M., Zaidan, W. and Rasheed, H. (2009), "Modeling of insulated CFRP-strengthened reinforced concrete T-beam exposed to fire", *Eng. Struct.*, **31**, 3072-3079.
- Huang, Z. (2010), "Modelling the bond between concrete and reinforcing steel in a fire", *Eng. Struct.*, **32**, 3660-3669.
- Huang, Z., Burgess, I. and Plank, R. (2006), "Behaviour of reinforced concrete structures in fire", *Structures in Fire, Fourth International Workshop*, Aveiro, May.
- ISO 834 (1975), Fire Resistance Test-Elements of Building Construction, International Standard 834
- Jiang, J. and Usmani A. (2013), "Modeling of steel frame structures in fire using OpenSees", *Comput. Struct.*, **118**, 90-99.
- Jiang, Y., Usmani, A. and Welch, S. (2011), "Development of heat transfer modelling capability in OpenSEES for structures in fire", *Application of Structural Fire Design*, Prague, April.
- Klingsch, E. (2014), "Explosive spalling of concrete in fire", Ph.D. Dissertation, Institut für Baustatik und Konstruktion, ETH Zürich, Switzerland
- Kodur, V. and Agrawal, A. (2016), "An approach for evaluating residual capacity of reinforced concrete beams exposed to fire", *Eng. Struct.*, **110**, 293-306.
- Kodur, V., Naser, M., Pakala, P. and Varma, A. (2013), "Modeling the response of composite beam-slab assemblies exposed to fire", *J. Constr. Steel Res.*, **80**, 163-173.
- Lazarevska, M., Knežević, M., Cvetkovska, M., Ivanišević, N., Samardžioska, T. and Trombeva-Gavrilovska, A. (2012), "Fire-resistance prognostic model for reinforced concrete columns", *Građevinar*, **64**(7), 565-571.
- Lennon, T. and Moore, D. (2003), "The natural fire safety concept - Full-scale tests at Cardington", *Fire Saf. J.*, **38**, 623-643.
- Mirza, O. and Uy, B. (2009), "Behaviour of headed stud shear connectors for composite steel-concrete beams at elevated temperatures", *J. Constr. Steel Res.*, **65**, 662-674.
- Pakala, P. and Kodur, V. (2016), "Effect of concrete slab on the behavior of fire exposed subframe assemblies with bolted double angle connections", *Eng. Struct.*, **107**, 101-115.
- Talamona, D. and Franssen, J.M. (2005), "A quadrangular shell finite element for concrete and steel structures subjected to fire", *J. Fire Protect. Eng.*, **15**, 237-264.
- Tan, K.H. and Nguyen, T.T. (2013), "Structural responses of reinforced concrete columns subjected to uniaxial bending and restraint at elevated temperatures", *Fire Saf. J.*, **60**, 1-13.
- Thelandersson, S. (1982), "On the multiaxial behavior of concrete exposed to high temperature", *Nucl. Eng. Des.*, **75**, 271-282.
- William, K. and Warnke, E. (1974), "Constitutive model for the triaxial behaviour of concrete", *Concrete Struct. Subj. Triax. Stress.*, 1-30.
- Zhou, C. and Vecchio, F. (2005), "Nonlinear finite element analysis of reinforced concrete structures subjected to transient thermal loads", *Comput. Concrete*, **2**(6), 455-479.